5. Exploring Urea Phase Connectivity in Molded Flexible Polyurethane Foam Formulations Using LiBr as a Probe

5.1 Chapter Summary

Lithium bromide is incorporated in formulations based on molded flexible polyurethane foams in order to systematically alter the phase separation behavior and thus give insight into urea phase connectivity. The formulations of the materials generated were similar to those of molded flexible polyurethane foams except that a surfactant and a low molecular weight cross-linking agent (such as diethanol amine) were *not* utilized. The resulting materials were evaluated using the techniques of AFM, SAXS, and DSC. AFM and SAXS were used to demonstrate that the materials with and without LiBr were microphase separated and possessed average interdomain spacings of ca. 90 Å, typical of flexible polyurethane foams. AFM phase images also showed that incorporation of LiBr reduced the urea phase aggregation, which is known to take place in flexible polyurethane foams, and led to a more homogeneous distribution of the urea microdomains in the soft polyol phase. Addition of LiBr also decreased the regularity in segmental packing of the hard segments, as was noted using WAXS. DSC scans revealed that in spite of the significantly different morphologies noted for the samples with different LiBr contents, soft segment mobility, as reflected by its T_g, remained unaffected on including this additive at the concentrations investigated. Interaction of LiBr with diethyl ether (DEE), 1,3-dimethylurea (DMU) and a model urethane (1,3-dimethylcarbamate) (URET) was also estimated by quantum mechanical calculations (QMC) using Density-Functional-Theory (DFT). For DMU and URET, QMC indicated a strong interaction of the Li^+ ion with ether and carbonyl oxygens; and of the Br^- with the (N–H) protons. Interaction energies of Li^+ with DEE ($O\cdots\cdots Li^+$), URET ($C{=}O\cdots\cdots Li^+$), and DMU ($C{=}O\cdots\cdots Li^+$) complexes were calculated to be –201, –239 and –272 kJ/mole respectively. Interaction energies of DEE, URET and DMU complexes with LiBr were calculated to be –198, –620, and –691 kJ/mole respectively, suggesting that the interaction of the salt was predominantly with the hard segments (urea and urethane) and not with the polyether soft segments.

5.2 Introduction

Polyurethanes, here after abbreviated as PU in this chapter, are a broad class of materials that find applications in a number of areas including foams, elastomers, adhesives, sealants, and coatings.[1,2] By volume, the use of PUs as flexible foams accounts for more than 50% of total PU production[3], which are primarily utilized in the transportation, furnishing, and packaging industries. Controlling the cellular structure and particularly the solid-state microphase separated morphology of flexible PU foams provides these materials with varied softness or firmness, resilience, and density.

The mechanical properties of flexible PU foams are a strong function of the microphase separated morphology which results due to an incompatibility between soft flexible polyether (or polyester) segments and water-extended toluene diisocyanate (TDI) based hard segments. The formation of the hard segments via the reaction of water and TDI ('blow' reaction) also yields carbon dioxide, which helps to expand the foaming mixture, thus giving the foam its cellular structure. While the 80:20 2,4/2,6 TDI mixture and water are generally used to generate urea based hard segments, the usually utilized polyether segments are based on ethylene oxide (EO), propylene oxide (PO), or both kinds of repeating units. The 'gelation' reaction, in which an isocyanate group reacts with a terminal hydroxyl group of the soft segment, covalently bonds the hard segments with the soft segments. As the chemical reactions proceed, the degree of polymerization (N) increases, and the interaction parameter (χ) also becomes more positive. Such changes lead to the system surpassing thermodynamic boundaries, and results in the precipitation of hard segments into urea microdomains. This process of microphase separation has been followed in a study by Elwell et al using in-situ FTIR and SAXS measurements.[4]

In addition to the microphase separation discussed above, workers have also noted the presence of macrophase-separated urea rich structures in flexible PU foams commonly referred to as urea balls or urea aggregates.[5,6,7] These aggregates were first reported in a study by Armistead et al using the technique of TEM and were observed to be ca. 300 nm in size.[5] More recently, workers have tried to elucidate the structure and composition of the urea aggregates using the analytical technique of x-ray microscopy (XRM).[6,7] The formation of urea aggregates has been noted to be favored in slabstock foams as compared to molded foams with similar hard segment contents.[3] Polyols employed in molded foams possess higher EO:PO ratios and are EO

end-capped as compared to those utilized in slabstock technology. This leads to differences in their solubility behavior and reaction kinetics, thus altering the urea aggregation characteristics.

The issue of hard segment connectivity in linear PU elastomers has also been discussed in previous studies. Abouzahr and Wilkes investigated a series of segmented PU elastomers with hard segment contents varied as 15, 25, 35, and 45 wt%.[8] The authors suggested that at 15 and 25 wt% hard segment content, the hard segment domains were randomly dispersed in the continuous soft phase. However, for the higher hard segment contents (35 wt% and higher), the authors proposed the formation of an interlocking connected morphology of the hard segment domains. In another study, Seymour and Cooper also concluded that above a certain hard segment content, ca. 25 %, it is impossible, due to spatial limitations, to have discrete separated hard segment domains.[9]

The importance of hard segment connectivity and its influence on mechanical and related properties of flexible PU foams was implied in a study carried out by Kaushiva and Wilkes.[10,11] The workers observed that the addition of diethanol amine (DEOA), a cross-linking agent commonly utilized in molded flexible PU foams, led to changes in the association of the urea phase at different length scales. They observed using FTIR and WAXS that there was a loss in the bidentate hydrogen bonding as well as the local ordering of the urea hard segments on addition of DEOA.[10] SAXS and AFM suggested that incorporation of DEOA led to the formation of urea microdomains ca. 5 nm in size, as compared to the foam without DEOA in which the microdomains were present, but aggregated into ca. 50 nm size regions.[10,11] These changes in the microphase separation characteristics brought about as a result of addition of DEOA were thought to lead to lower load-bearing properties of the foams containing the cross-linking agent.[10]

Moreland and Wilkes investigated the effect of incorporating LiCl in a slabstock foam with an attempt to produce ‘softer’ foams which maintained high hard segment contents and thus eliminated the use of a physical blowing agent.[12] As expected, LiCl was found to disrupt the hydrogen bonding in the polymer, leading to foams in which a loss in the local ordering of the hard segments was observed (WAXS). In addition the authors also observed via TEM that the urea aggregation was suppressed on addition of this additive.

Extending the work done by Moreland and Wilkes, the author addressed the issue of urea phase connectivity in plaques based on *molded* flexible PU foams in Chapter 4. In that study, it

was demonstrated that materials with varied levels of urea phase connectivity could be obtained by incorporating lithium chloride as an additive in the formulation. The physical associations of the urea aggregates, or the *macro* connectivity was observed to be systematically reduced as the LiCl content was increased. Using WAXS, the authors also showed that LiCl disrupted the regularity in the segmental packing of the urea hard segments, leading to a loss in the *micro* level connectivity. In Chapter 3, the author also focused on using LiCl as an additive in *slabstock* foam formulations in order to understand the effect of urea phase connectivity on mechanical and viscoelastic properties. The materials containing LiCl were noted to display higher rates of stress-relaxation as compared to the materials that did not contain the additive. It was suggested that since LiCl considerably reduced the bidentate hydrogen bonding of the urea hard segments, there was more chain slippage in materials containing the additive, which led to the observed increase in the rate of stress-relaxation. The author also observed that the modulus values obtained at ambient conditions were a stronger function of LiCl content when the hard segment content was higher. This observation further reinforced the idea that hard segment connectivity, due to volume fraction arguments, plays a stronger function on the structure-property relationships when the hard segment content is relatively high.

The present study investigates the use of another lithium salt – lithium bromide, to probe hard segment connectivity in formulations based on molded flexible PU foams. It will be shown in this report that the results which have been noted in the Chapters 3 & 4 using LiCl are not unique to LiCl, but other salts such as LiBr also present opportunities to probe hard segment connectivity in flexible PU foams by impeding their hydrogen bonding characteristics. Yilgor et al have demonstrated that the strength of hydrogen bonding interactions in PUs can be quantified using semi-empirical quantum mechanical calculations (QMC) using a density functional theory (DFT).[13] QMC is a valuable technique to determine the interaction energies and the stabilities of complexes formed between model compounds due to hydrogen bonding, ionic interactions, dipole-dipole or other types of electrostatic interactions. It is also possible to construct vibrational spectra of single molecules or complexes and determine the magnitude of peak shifts as a result of complexation, using QMC. Theoretical vibrational spectra have been shown to be in very good agreement with the experimental spectra.[14] In the present study, QMC will be utilized to probe the competitive interaction of the urea and urethane based hard segments and the polyether soft segments with LiBr.

5.3 Experimental

5.3.1 Materials

The samples investigated in this study were prepared at Dow Chemical in Freeport, TX. The materials employed Voranol 4703®, which is a commercial grade polyol used in the production of molded flexible PU foams. The equivalent weight of this polyol is 1667 and it possesses an average functionality of 2.50. Since molded foams typically require fast reaction times, this EO/PO (ethylene oxide / propylene oxide) based polyol is EO end-capped and possesses an EO:PO ratio of 16:84. All formulations were based on a TDI index of 100 and a 4.5 parts per hundred polyol (pphp) water content. This corresponds to the materials possessing ca. 30.9 wt% hard segments. The catalyst package, which was used at a level of 0.2 pphp, consisted of 5 parts by weight of Dabco 33LV for each part of Dabco BL11. Specific details regarding the catalysts can be found elsewhere.[3] The LiBr content was varied in a systematic manner as 0.0, 0.1, 0.2, 0.5, 1.0, and 1.5 pphp to match the LiCl contents used in the study carried out previously in the same laboratory and described in Chapter 4.

The preparation of the samples was carried out in a lab scale cup-foaming setup. Water (with a known amount of dissolved LiBr), and the polyol, were added to a cup and the mixture was stirred for 25 seconds at 2000 rpm with a 1" diameter stirrer. The TDI and the catalyst were then added and the mixture was stirred for another 15 seconds. The foam formation was suppressed by forcing the foam to collapse by stirring. While the foaming reactions were occurring, a small amount of the foaming mixture (ca. 50 mg) was removed from the cup and placed on a clean glass slide. A doctor blade was then used to cast a ca. 50 μm film. The glass slide was then placed in an oven operating at 100 °C for 1 hour in order to facilitate completion of the reactions.

5.3.2 Methods

Tapping mode atomic force microscopy (AFM) scans were performed on a Digital Instruments Scanning Probe Microscope employing a Nanoscope IIIa controller and Nanosensors TESP (Tapping Etched Silicon Probe) type single beam cantilevers. These experiments were carried out to investigate the urea aggregation behavior as well as to evaluate the presence, size, and dispersion of nanoscopic level structures. The cantilevers typically used have a nominal length of 125 μm, force constants in the range of 35 ± 7 N/m, and oscillation

frequencies of the order of 260–320 kHz. The free air oscillation amplitude was set at 60 nm, and the amplitude of the tip while tapping the surface was maintained at ca. 58 % of this value. In addition to phase images, height images – which are based on changes in surface topography, were also collected, but these images will not be presented. In phase images obtained by *t*-AFM, a higher modulus material typically induces a higher phase offset and appears lighter as opposed to a softer phase, which appears darker. Thus, for the PUs imaged in this investigation, the urea rich regions appear lighter where as darker regions correspond to the softer polyol phase.

To investigate the local ordering of the hard segments at the 1-10 Å level, wide angle x-ray scattering (WAXS) was employed. SAXS was utilized to compare the interdomain spacing with that obtained using analysis of AFM images, as discussed later. The procedures for these experiments have been used routinely and have been described in previous chapters.

Differential scanning calorimetery (DSC) experiments were conducted using a Seiko DSC 220C under a nitrogen purge and at a heating rate of 10°C/min. Small amounts (6-8 mg) of the cast films were scraped from the glass slides in order to carry out these experiments. The DSC curves were normalized to a 1 mg sample mass. DSC was carried out to observe any changes in the soft segment glass transition position and breadth on addition of LiBr.

Gaussian98, revision A.6, was used to determine stabilities of complexes from full optimization of all geometrical parameters.[15] Density-functional-theory (DFT) formalism with three-parameter hybrid-functional of Becke has been employed.[16] The basis set chosen was 6-31G(d,p). Zero-point energy corrections did not change the results significantly, so they have been neglected in this report. Similarly, the corrections to the basis set superposition errors are not included in the calculations. Computation of the interaction energy between various donor-acceptor pairs goes through a super-molecule approach where the ground state energy of the complex ($E_{COMPLEX}$) is calculated and compared to the sum of the ground state energies (E_1+E_2) of the individual components. The interaction energy for the complex, also referred to as the stability of the complex, is then determined as $E_{STABILITY} = (E_1+E_2) - E_{COMPLEX}$.

5.4 Results and Discussion

Tapping mode AFM is now a well established technique to characterize the fine structure of PU materials. Studies carried out by McLean et. al.[17] and Garrett et. al.[18] in the area of PU elastomers; and also the work of Kaushiva et. al.[11,19] and the present authors work in Chapters 3

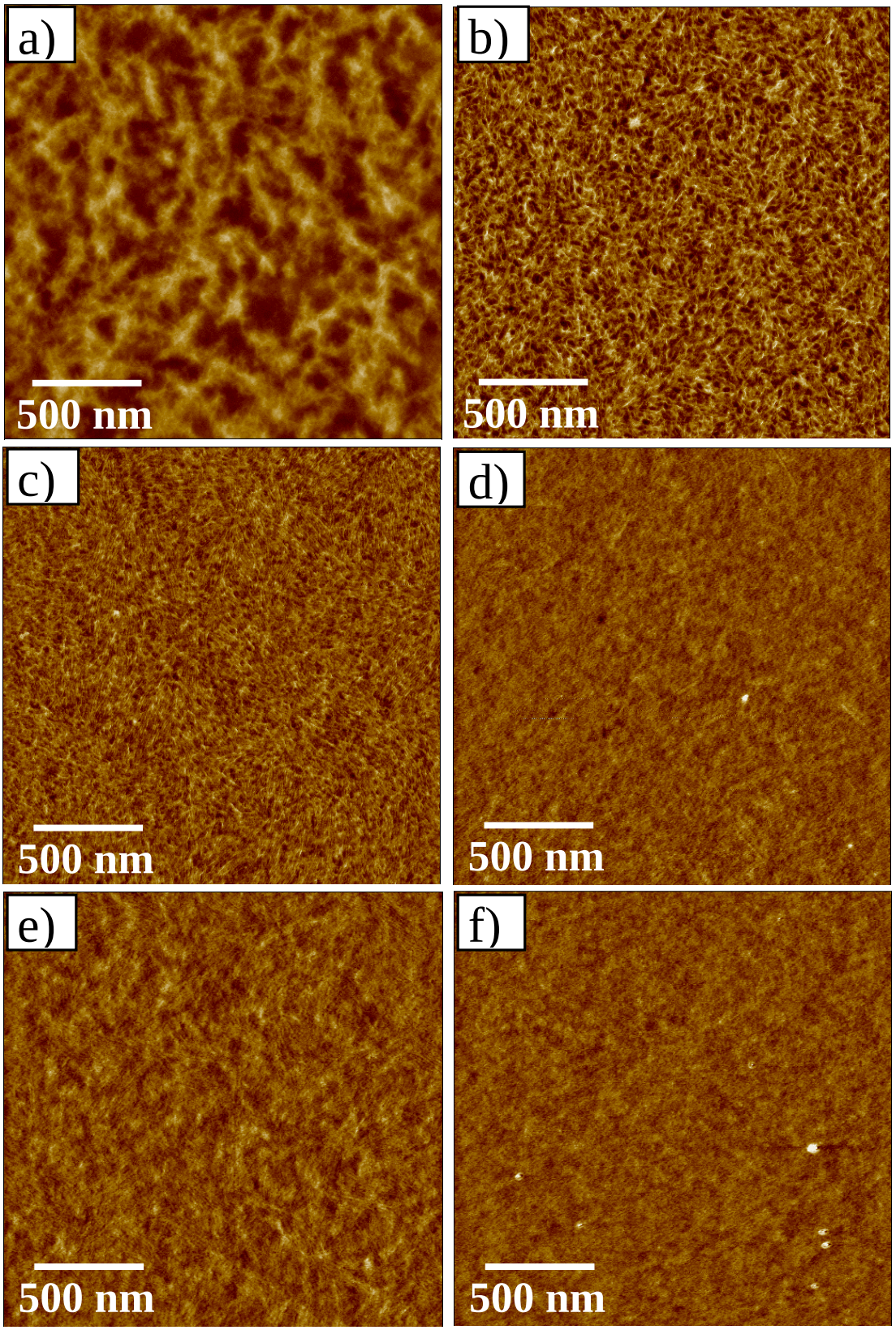

Figure 5.1 Atomic force microscopy phase images for samples with varying LiBr content: a) 0.0 LiBr pphp, b) 0.1 LiBr pphp, c) 0.2 LiBr pphp, d) 0.5 LiBr pphp, e) 1.0 LiBr pphp, and f) 1.5 LiBr pphp.

& 4 on PU foam materials have successfully elucidated their microphase separated morphology. AFM also has the advantage of being a relatively easier technique, as compared to TEM, to obtain valuable high magnification information at the microdomain level.

Tapping mode AFM phase images (2 x 2 μm^2) for the samples investigated in the current study are presented in Fig 5.1. It is observed that all the materials are microphase separated since all images display a phase contrast between the harder urea phase and the softer polyol phase. No directional dependence was observed as a result of casting the films using a doctor blade. The AFM image of the sample which does not contain LiBr (Fig 5.1(a)) displays urea rich regions, or urea aggregates, of the order of 100-200 nm. These regions are thought to arise from the aggregation of the urea microdomains. On addition of even a small amount of LiBr (0.1 LiBr pphp), the level of aggregation of the urea microdomains is decreased and the AFM image corresponding to this formulation (Fig 5.1(b)) displays urea rich regions which are ca. 50-100 nm in size. Further increasing the level of LiBr to 0.2 pphp leads to a further reduction in the associations of the urea microdomains resulting in urea rich regions, which are typically smaller than 50 nm in size. On increasing LiBr content to even higher levels, a further reduction in the size of the urea rich regions is observed and at 0.5, 1.0, and 1.5 LiBr pphp these urea rich regions are believed to be close to the microdomain size. It is also observed that the size of the polyol rich regions (the darker regions in the images) is found to systematically reduce on increasing the LiBr content. The results presented in this set of AFM images show similar trends to those observed in the earlier work reported in Chapter 4 which utilized LiCl as an additive.

Phase images of polymers have been numerically examined in the past by workers to quantify any periodically occurring structure at the surface of the material.[17,19] This is done using a Fourier transform analysis of the surface characteristics and is also often called the power spectral density (PSD).[20] This analysis technique characterizes the material by assigning a wavelength to any periodically occurring structure. Thus the wavelengths which occur the most frequently appear as peaks or spikes in the distribution. In Fig 5.2a, the power spectral density profile of an arbitrarily chosen sample from the present series, containing 1.0 LiBr pphp, reveals a periodically occurring wavelength in the phase image. This observed maximum, which occurs at ca. 90 Å, is thought to be representative of the interdomain spacing typically observed in these materials via small angle x-ray scattering (SAXS). Fig 5.2b shows the SAXS profile for the same sample containing 1.0 LiBr pphp and displays an interdomain spacing of ca. 85 Å, in good

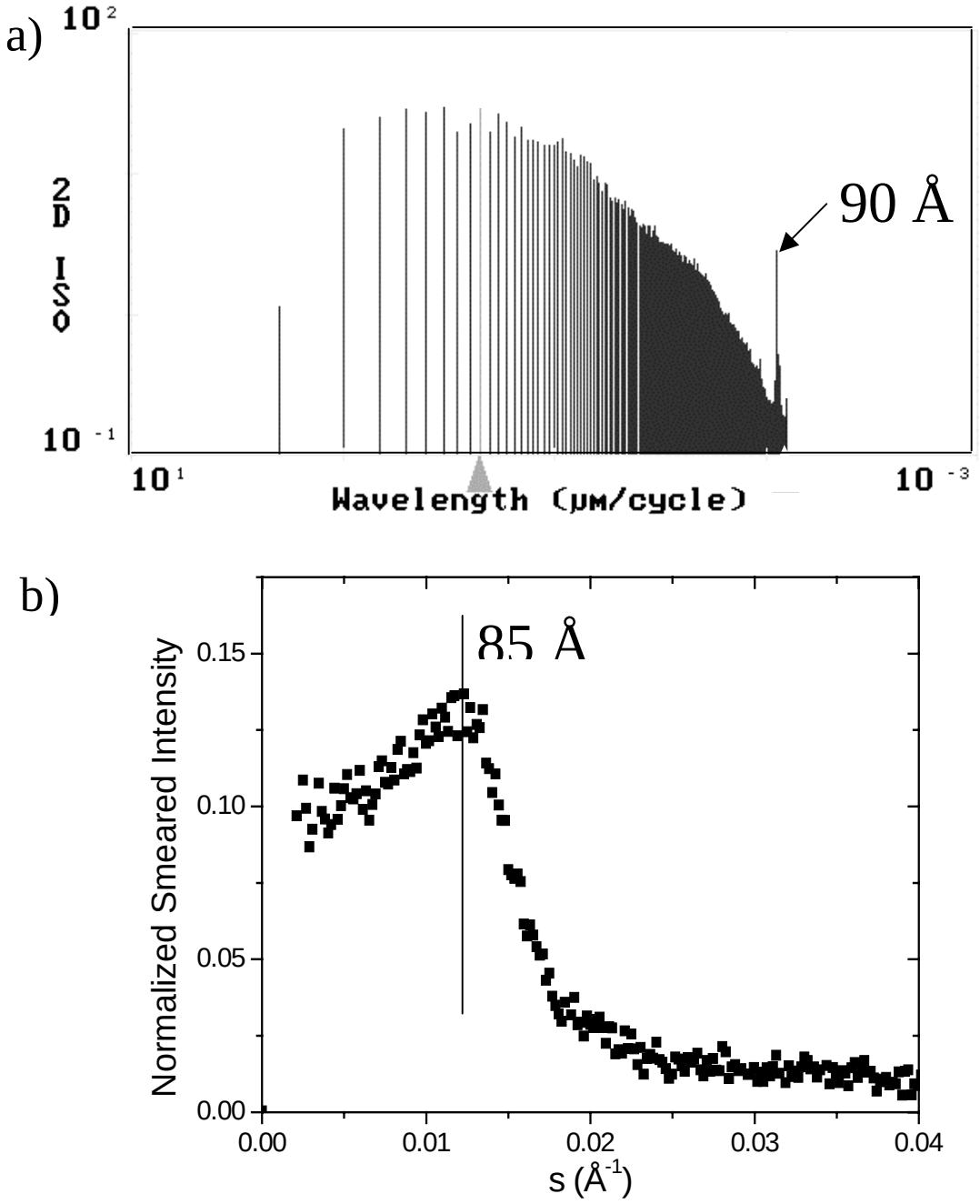

Figure 5.2 Comparison of interdomain spacing obtained from a) PSD analysis of AFM phase image, and b) SAXS for the sample containing 1.0 LiBr pphp.

agreement with the PSD data. The PSD analysis of other samples from the present series showed that the interdomain spacing remains relatively unchanged at ca. 90 Å, irrespective of LiBr content. This result is in agreement with a previous study (Chapter 4), where the author showed via SAXS that addition of LiCl in a series of plaques based on molded flexible PU foams, the interdomain spacing also remained unchanged at ca. 100 Å.

The ordering of the hard segments can be detected as a 4.7 Å reflection using WAXS, and is well documented.[5,10,19] The sample which did not contain LiBr displayed a weak but distinct 4.7 Å reflection. This reflection was found to be absent in the samples containing LiBr, suggesting that the regularity in the packing behavior was reduced on addition of the additive. The WAXS data is not presented here for brevity.

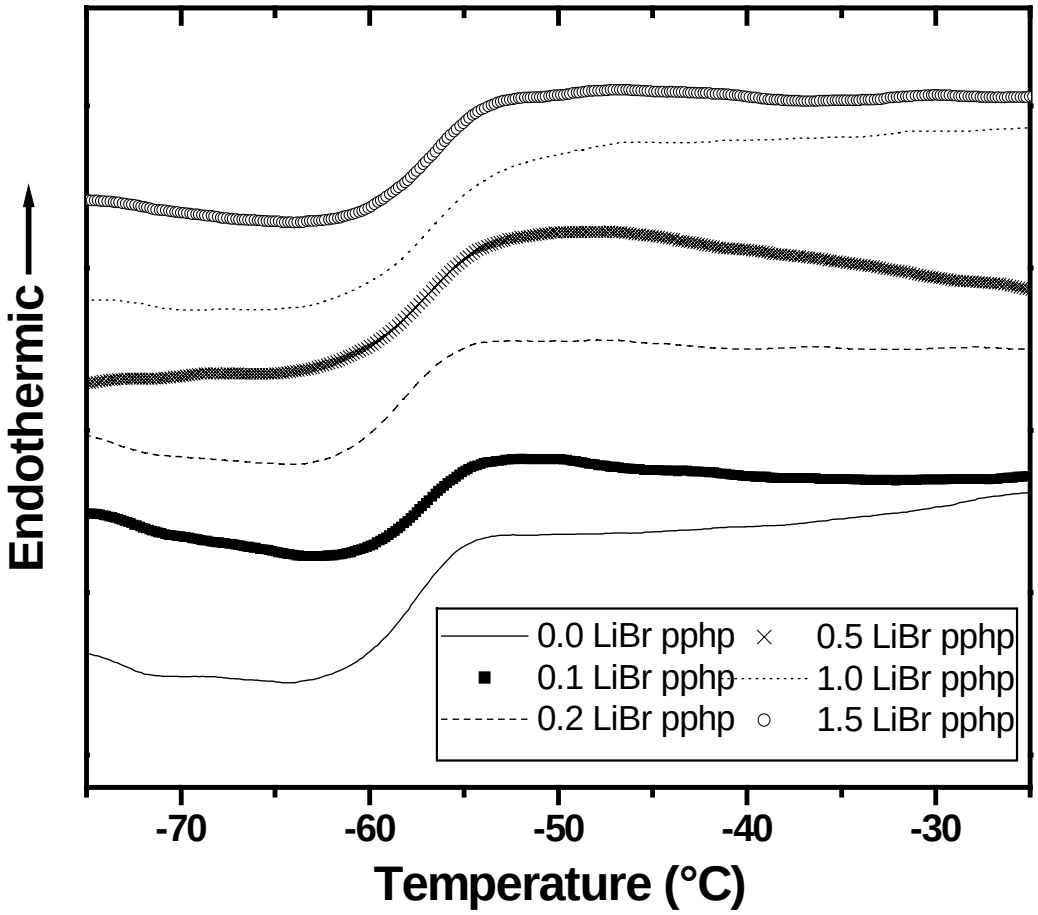

Figure 5.3 Soft segment glass transition observed via DSC for the present series with varied LiBr content.

The DSC curves for all the six samples investigated are presented in Fig 5.3. DSC was utilized to ascertain the influence of LiBr on soft segment mobility. It is clearly observed on inspection of Fig 5.3, that all six materials exhibit a soft segment glass transition at ca. –58 °C, in agreement with previously reported values for flexible PU foam materials.[3,5] The same figure also reveals that the soft segment glass transition breadth, as well as position, remain relatively constant for all the six samples examined. *This observation implies that although there occur*

considerable changes in the nature of microphase separation on incorporation of LiBr, as observed via AFM, the soft segment mobility remains unaffected on including this additive.

In light of the fact that AFM, SAXS, and WAXS show significant changes in the morphology of the hard phase on LiBr addition, it is thought that the LiBr interacts preferentially with the urea/urethane moieties. The soft segment T_g remaining unchanged is another indication that there is no pronounced interaction of LiBr with the soft phase. In order to better understand

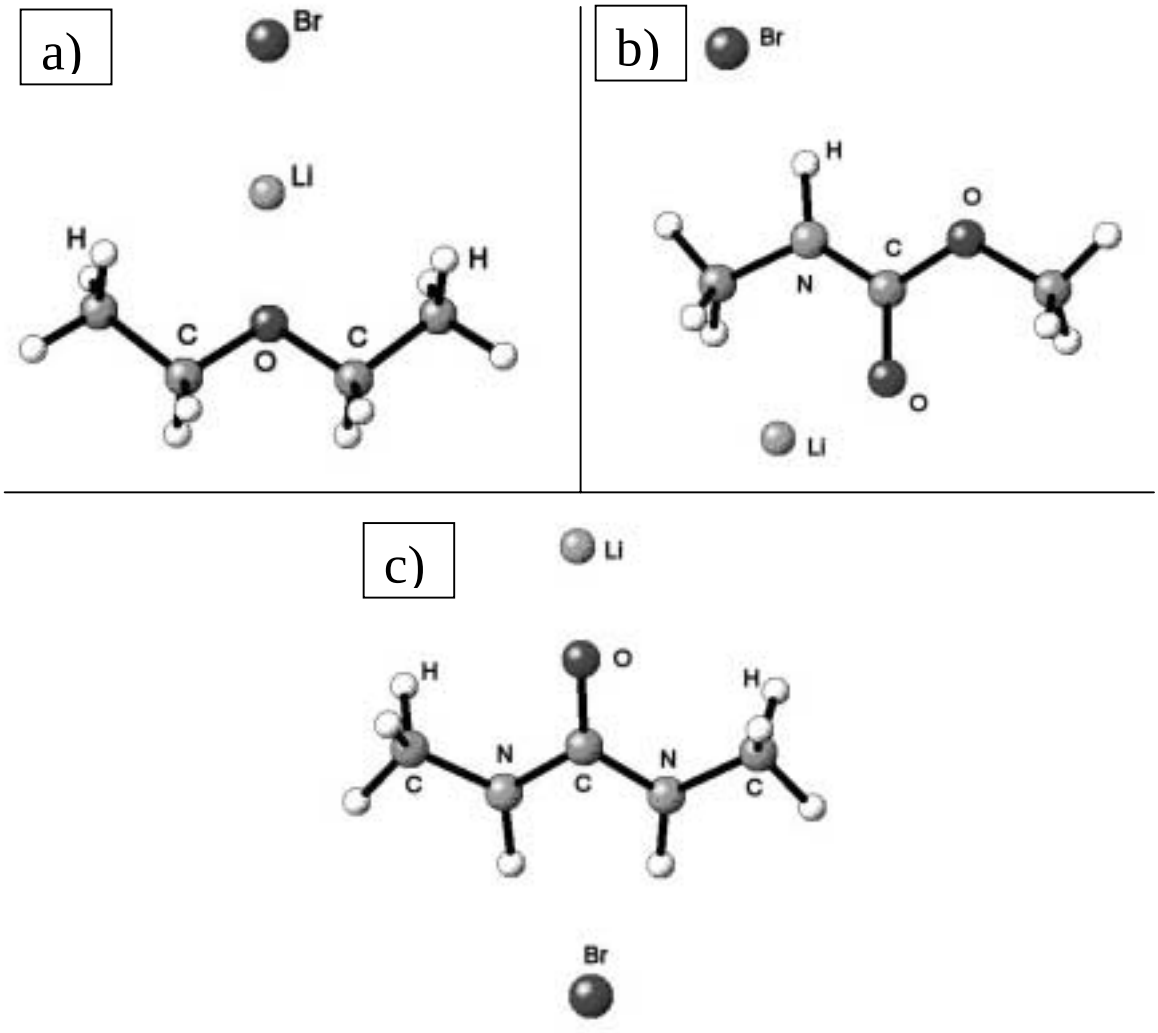

Figure 5.4 Theoretically predicted molecular geometries from DFT calculations a) DEE–LiBr complex, b) URET – LiBr Complex, and c) DMU – LiBr complex.

this behavior, advanced quantum mechanical calculations were performed on model systems, where interaction geometries and interaction energies of the complexes formed between LiBr and model urea, urethane, and ether compounds were determined. In addition to the interaction energies, it is also important to take into account the ionic radii and volumes of Li^+ and Br^- ions

when considering their influence on packing behavior of hard segments and as a result on the overall morphology of the system. Li^+ has an ionic radius of 0.6 Å and molar volume of 0.55 cm^3/mol, whereas Br^- has an ionic radius of 1.96 Å and molar volume of 19.0 cm^3/mol. This compares to the ionic radius of Cl^- (15.0 cm^3/mol) which has been used in a previous study by the present authors.[21] Molar volumes of diethylether (DEE), 1,3-dimethylcarbamate (URET) and 1,3-dimethylurea (DMU) were determined to be 80.7, 77.9 and 70.4 cm^3/mol respectively, determined by the group contribution method.[22,23] The volume of Br^- is approximately 35 times larger than that of Li^+ and as a result is expected to disrupt the packing in the urea segments dramatically.

Figs 5.4a – 5.4c give the geometries of the most stable complexes formed between LiBr and DEE, URET and DMU respectively. The most significant difference between DEE–LiBr (Fig 5.4a) and URET–LiBr and DMU–LiBr complexes (Figs 5.4b and 5.4c) is the position of the Br^- ion in the system. It is clear that Br^- prefers to stay as far away as possible from the ether backbone (4.09 Å) since it cannot be stabilized by ether hydrogens. On the other hand, as clearly shown in Figs 5.4b and 5.4c, both Li^+ and Br^- ions are involved in the URET and DMU complexes. Li^+ interacts with carbonyl oxygen, whereas Br^- complexes with (N–H) protons of

System	Stabilization energy (kJ/mol)	O·····Li^+ (Å)	H····· Br^- (Å)
DEE–Li+	–201	1.81	–
URET–Li+	–239	1.73	–
DMU–Li+	–272	1.71	–
DEE–Br–	3	–	
URET–Br–	–371	–	
DMU–Br–	–419	–	
DEE–LiBr	–198	1.87	4.09
URET–LiBr	–620	1.76	2.02
DMU–LiBr	–691	1.66	2.2

Table 5.1 Quantum mechanical calculations on the interaction of Li^+, Br^- and LiBr with model compounds, 1,3-dimethylurea (DMU), 1,3-dimethlycarbamate (URET) and diethyl ether (DEE). Bond lengths and stabilization energies of the complexes formed.

urea or urethane. The distances of Br^- from the protons of URET and DMU are 2.02 and 2.20 Å respectively, much shorter than that of DEE. This result obtained from QMC strongly supports the experimental observations regarding the preferential interaction of LiBr with urea groups but not with the polyether backbone. It is also interesting to note in Fig 5.4c that Br^- forms a dihedral complex with DMU, similar to the hydrogen bonding between urea groups. Table 5.1 provides the interaction energies and various bond distances for all the complexes investigated. As expected, Li^+ ions show the strongest interaction with (C=O) in DMU, which has a stability energy of –272 kJ/mol, followed by (C=O) in URET with an energy of –238 kJ/mol. The weakest interaction is observed in the DEE–Li^+ complex, where the stability energy is only –201 kJ/mol. Substantial influence of the Br^- counterion on the complexes formed can clearly be seen from the stabilization energies of DEE–LiBr, URET–LiBr and DMU–LiBr, which are –198, –620 and –691 kJ/mol respectively. As shown in Table 5.1, by subtracting the energies of Li^+ complexes from the energy of the respective LiBr complex, it is possible to estimate the contribution of the Br^- ion to the stabilization of these systems. When this is done, it is interesting to note that DEE–LiBr complex turns out to be less stable than the DEE–Li^+ complex by about (+3 kJ/mol). On the other hand the Br^- ion contributes strongly to the stabilization of the URET–LiBr (–371 kJ/mol) and DMU–LiBr (–419 kJ/mol) complexes. Results obtained from QMC on the stabilities of these complexes clearly show that LiBr will preferentially interact with urea or urethane groups, but not with the ether group. This could lead to the disruption of hydrogen bonding between hard segments and therefore would negatively influence the order and packing of these hard segments. This theoretical observation provides direct support to the experimental observations already discussed earlier in this paper.

5.5 Conclusions

Lithium bromide was used as an additive to probe urea based hard segment connectivity in formulations based on molded flexible PU foams. AFM showed that the incorporation of LiBr was found to systematically reduce the aggregation of the urea phase, and led to a loss in the connectivity at the urea aggregate level. AFM also revealed that the average interdomain spacing remained unaltered at ca. 90 Å irrespective of LiBr content. WAXS showed that addition of LiBr prevented the hard segments to arrange in a regular manner, resulting in a loss in inter-segmental connectivity. DSC was utilized to study the behavior of the soft segment glass transition in

formulations with and without LiBr. It was observed that the soft segment mobility remained relatively unchanged on addition of LiBr in the range of LiBr contents investigated. These observations support the findings made in Chapter 4 by the author, which incorporated LiCl as an additive in similar formulations. Experimental results were shown to be in good agreement with quantum mechanical interactions, which clearly show very strong interaction of LiBr with urea and urethane groups, as compared to diethyl ether. These ion-dipole interactions are much stronger than the hydrogen bonding interaction between two adjacent urea or two adjacent urethane groups.[14] This interaction in turn leads to disruption of hydrogen bonding between urea groups in the system. Fairly large bromide (Br^-) counterions also contribute to disruption of the ordering of the urea phase.

There are a number of variables, which can affect hard segment connectivity in flexible PU foams. Some of these variables could be the hard segment content, type of polyol, type of isocyanate and its symmetry, inclusion of certain additives and cross-linking agents. The present study using LiBr, and the previous studies using LiCl (Chapters 3 & 4), are a step towards understanding urea phase connectivity and the opportunities it presents in tailoring the mechanical and related properties of flexible PU foams.

5.6 References

1. Woods, G. The ICI Polyurethanes Book, 2nd ed.; ICI Polyurethanes and John Wiley and Sons: 1990.
2. Hepburn, C. Polyurethane Elastomers, 2nd ed.; Elsevier Applied Science: London, 1991.
3. Herrington, R.; Hock, K. Flexible polyurethane foams, 2nd ed.; Dow Chemical Co.: Midland, MI, 1998.
4. Elwell, M.J.; Ryan, A.J.; Grünbauer, H.J.M.; Van Lieshout, H.C. Macromolecules 1996, 29, 2960.
5. Armistead, J.P.; Wilkes, G.L.; Turner, R.B. J Appl Polym Sci 1988, 35, 601.
6. Ade, H.; Smith, A.P.; Cameron, S.; Cieslinski, R.; Mitchell, G.; Hsiao, B.; Rightor, E. Polymer 1995, 36, 1843.
7. Rightor, E.G.; Urquhart, S.G.; Hitchcock, A.P.; Ade, H.; Smith, A.P.; Mitchell, G.E.; Priester, R.D.; Aneja, A.; Appel, G.; Wilkes, G.L.; Lidy, W.E. Macromolecules (in press)
8. Abouzahr, S.; Wilkes, G.L.; Ophir, Z. Polymer 1982, 23, 1077.
9. Seymour, R.W.; Cooper, S.L. Adv Urethane Sci 1974, 3, 66.
10. Kaushiva, B.D.; Wilkes, G.L. J Appl Polym Sci 2000, 77, 202.
11. Kaushiva, B.D.; Wilkes, G.L. Polymer Commun 2000, 41, 6981.
12. Moreland, J.C.; Wilkes, G.L.; Turner, R.B.; Rightor, E.G. J Appl Polym Sci 1994, 52, 1459.

13. Yilgor, E.; Burgaz, E.; Yurtsever, E.; Yilgor, I. Polymer 2000, 41, 849.
14. Yilgor, E.; Yilgor, I.; Yurtsever, E. submitted to Polymer.
15. Gaussian 98, Revision A.6, Frisch, M.J.; Trucks, G.W.; Schlegel, H.B.; Scuseria, G.E.; Robb, M.A.; Cheeseman, J.R.; Zakrzewski, V.G.; Montgomery, Jr. J.A.; Stratmann, R.E.; Burant, J.C.; Dapprich, S.; Millam, J.M.; Daniels, A.D.; Kudin, K.N.; Strain, M.C.; Farkas, O.; Tomasi, J.; Barone, V.; Cossi, M.; Cammi, R.; Mennucci, B.; Pomelli, C.; Adamo, C.; Clifford, S.; Ochterski, J.; Petersson, G.A.; Ayala, P.Y.; Cui, Q.; Morokuma, K.; Malick, D.K.; Rabuck, A.D.; Raghavachari, K.; Foresman, J.B.; Cioslowski, J.; Ortiz, J. V.; Stefanov, B.B.; Liu, G.; Liashenko, A.; Piskorz, P.; Komaromi, I.; Gomperts, R.; Martin, R.L.; Fox, D.J.; Keith, T.; Al-Laham, M.A.; Peng, C.Y.; Nanayakkara, A.; Gonzalez, C.; Challacombe, M.; Gill, P.M.W.; Johnson, B.; Chen, W.; Wong, M.W.; Andres, J.L.; Gonzalez, C.; Head-Gordon, M.; Replogle, E.S.; Pople J.A.; Gaussian, Inc., Pittsburgh PA, 1998.
16. Becke, A.D.; J. Chem. Phys. 1996, 104, 1040.
17. McLean, R.S.; Sauer, B.B. Macromolecules 1997, 30, 8314.
18. Garret, J.T.; Runt, J.; Lin, J.S. Macromolecules, 2000, 33, 6353.
19. Kaushiva, B.D.; McCartney, S.R.; Rossmy, G.R.; Wilkes, G.L. Polymer, 2000, 41, 285.
20. Nanoscope III command reference manual. Update Version 4.10, Digital Instruments Nanoscobe scanning probe microscobes. Auigust 1995, pp.12.52-12.60.
21. Aneja, A.; Wilkes, G.L.; Yurtsever, E.; Yilgor, I. manuscript in preparation.
22. Van Krevelen, D.W.; Properties of Polymers, Elsevier, Amsterdam, 1990, Ch. 7.
23. Porter D., Group Interaction Modeling of Polymers, Marcel Dekker, New York, 1995.